AGU PUBLICATIONS

Paleoceanography

RESEARCH ARTICLE
10.1002/2013PA002589

**Key Points:**
- Coccolith Sr/Ca reveals productivity on Agulhas Bank slope
- Southern Hemisphere westerlies controlled paleoproductivity on the Agulhas Bank
- Productivity records from the area provide information on westerly dynamics

**Supporting Information:**
- Readme
- Figure S1
- Figure S2
- Figure S3
- Figure S4
- Figure S5
- Figure S6

**Correspondence to:**
L. M. Mejía,
luzmamera2@yahoo.com

**Citation:**
Mejía, L. M., P. Ziveri, M. Cagnetti, C. Bolton, R. Zahn, G. Marino, G. Martínez-Méndez, and H. Stoll (2014), Effects of midlatitude westerlies on the paleoproductivity at the Agulhas Bank slope during the penultimate glacial cycle: Evidence from coccolith Sr/Ca ratios, *Paleoceanography*, *29*, 697–714, doi:10.1002/2013PA002589.

Received 5 DEC 2013
Accepted 27 MAY 2014
Accepted article online 3 JUN 2014
Published online 2 JULY 2014

# Effects of midlatitude westerlies on the paleoproductivity at the Agulhas Bank slope during the penultimate glacial cycle: Evidence from coccolith Sr/Ca ratios

**Luz María Mejía[1], Patrizia Ziveri[2,3], Marilisa Cagnetti[2], Clara Bolton[1], Rainer Zahn[2,4], Gianluca Marino[2,5], Gema Martínez-Méndez[2,6], and Heather Stoll[1]**

[1]Departamento de Geología, Universidad de Oviedo, Oviedo, Asturias, Spain, [2]Institut de Ciència i Tecnologia Ambientals, Universitat Autònoma de Barcelona, Catalonia, Spain, [3]Department of Earth Sciences, Vrije Universiteit Amsterdam, Amsterdam, Netherlands, [4]ICREA (Institució Catalana de Recerca i Estudis Avançats), Passeig Lluís Companys 23, Barcelona, Spain, [5]Now at Research School of Earth Sciences, Australian National University, Canberra, ACT, Australia, [6]Now at MARUM-Center for Marine Environmental Sciences, University of Bremen, Bremen, Germany

**Abstract** Modern primary productivity on the Agulhas Bank, off South Africa, has been proposed to be linked to the midlatitude westerlies. A paleoproductivity record from this area may therefore resolve temporal changes in the westerly dynamics. Accordingly, we produced a coccolith Sr/Ca-based paleoproductivity record from core MD96-2080 (Agulhas Bank slope) during the penultimate glacial-interglacial cycle. Deriving the productivity signal from Sr/Ca requires a correction for a temperature effect, here constrained using Mg/Ca sea surface temperatures from the foraminifer *Globigerina bulloides* from core MD96-2080. Phases of depressed productivity coincided with periods of stratification in the same core, indicated by high relative abundances of the coccolithophore *Florisphaera profunda* and with low relative abundances of the upwelling indicator *G. bulloides* in the nearby Cape Basin. These observations collectively suggest that productivity was regulated by upwelling throughout this region. We infer that, as in the present, periods of low productivity result from a more northerly position of the westerlies, potentially accompanied by subtropical front displacements, and blockage of upwelling promoting easterlies. Productivity minima also coincide with periods of increased ice-rafted detritus (IRD) deposition on the Agulhas Plateau, which also indicates extreme northward positions of the westerlies. The influence of the westerlies appears to be obliquity conditioned, as productivity minima (and IRD maxima) occur during low-obliquity intervals. The dynamic connection between productivity and the westerlies is supported by coeval salinity changes in the South Indian Gyre that likewise respond sensitively to a poleward contraction of the westerlies.

## 1. Introduction

Contrasting hypotheses on past dynamics of Southern Hemisphere midlatitude westerly winds derived from several different proxies and models [e.g., *Kohfeld et al*., 2013; *Sime et al*., 2013] hamper our ability to understand past westerly wind influence on key processes that have driven important climatic changes, such as atmospheric partitioning of $CO_2$ over glacial-interglacial cycles [*Toggweiler et al*., 2006; *Anderson et al*., 2009]. For instance, variation of the latitudinal position and/or strength of westerlies have been suggested to contribute to Southern Ocean productivity variations [*Kohfeld et al*., 2013] and Circumpolar Deep Water (CDW) ventilation [*Toggweiler et al*., 2006; *Anderson et al*., 2009], which both in turn regulate atmospheric $CO_2$ concentrations. However, recent reviews such as that of *Kohfeld et al*. [2013] and models [*Sime et al*., 2013] reveal that existing data are not strongly diagnostic of a more equatorward position of the westerlies during cold periods, and other mechanisms or combinations of mechanisms also offer compatible explanations for the available observations [*Kohfeld et al*., 2013]. Given the current uncertainties in reconstructions of past westerly wind dynamics, a proxy able to provide information on past variability in the latitudinal displacement and/or intensity of the westerlies would clarify their role in late Quaternary climate variations.

Modern productivity in the Agulhas Bank region (Atlantic sector of the Indian-Atlantic oceanic gateway, South African margin) appears tightly coupled to the location of the Southern Hemisphere midlatitude westerly wind belt [*Schumann et al*., 1995; *Jury*, 2011]. During austral winters, when westerlies are located at

their northernmost position, they block the influence of easterly trade winds responsible for upwelling. During austral summers, the poleward retreat of the westerlies allows influence of the easterly trade winds that promote upwelling and water mixing processes, driving increased productivity [*Jury*, 2011]. When this typical seasonal pattern is disrupted by westerlies located unusually north during austral summer, easterly trade winds exert less influence on the Agulhas Bank region, and nutrients are not upwelled [*Schumann et al*., 1995], decreasing average productivity. Assuming that the latitudinal position of westerlies was also the main regulator of productivity in the past, a paleoproductivity record from the Agulhas Bank slope could serve as a proxy to trace the past behavior of the westerly wind belt in the Southern Hemisphere.

Most studies to date have focused on the potential role of varying westerly position and/or intensity at the Last Glacial Maximum (LGM), and fewer investigations have explored the temporal pattern of change in westerlies or their role in the penultimate glacial cycle. Therefore, in this study, we focus on reconstructing productivity from core MD96-2080, on the Agulhas Bank slope (Figure 1), during the penultimate glacial-interglacial cycle (i.e., between 216 and 116 kyr), with the aim of providing new information that may resolve the temporal pattern of variability in the location of the westerly wind belt.

We employ as a productivity indicator the Sr/Ca ratio of coccoliths. Coccolith geochemistry-based productivity indicators have the advantage of recording the surface water signal. They therefore remain independent of changes in preservation potentially related to bottom water carbonate undersaturation or oxygenation that strongly affect accumulation rate-based productivity proxies and which might result from changing (northern versus southern) deepwater sources over glacial-interglacial cycles [e.g., *Martínez-Méndez et al*., 2008, 2009]. Coccolith Sr/Ca is a relatively recent approach to reconstructing paleoproductivity. It is based on consistent positive correlations between coccolith Sr/Ca and nutrient-stimulated changes in coccolithophore productivity in culture, sediment core top, and sediment trap studies [*Rickaby et al*., 2002; *Stoll et al*., 2002b, 2002c, 2007c]. Although the mechanism linking Sr incorporation to productivity has not been identified in detail, one hypothesis is that nutrient limitation in coccolithophores triggers excretion of extracellular polysaccharides which preferentially bind extracellular Sr and depress the Sr/Ca ratio of ions transported to the calcification vesicle [*Langer et al*., 2006]. A comparison of Quaternary coccolith Sr/Ca downcore records [*Stoll et al*., 2007b] with other productivity indicators suggests a persistent relationship between coccolith Sr/Ca and productivity. A secondary influence of temperature on Sr/Ca was observed in culture studies [*Stoll et al*., 2002a] and can be removed from paleoproductivity records using independent estimates of calcification temperature (e.g., foraminiferal Mg/Ca) from the same core. To verify that changes in species' composition do not affect the measured trends in coccolith Sr/Ca, we have also characterized coccolith assemblages in the sediment in the exact same samples. Our new productivity record derived from coccolith Sr/Ca was integrated with other regional records that reflect productivity, providing novel insights into past Southern Hemisphere midlatitude westerly behavior and revealing new perspectives on its response to orbital forcing.

## 2. Site Location and Oceanographic Setting

### 2.1. Core Location, Chronology, and Modern Hydrography

Core MD96-2080 was obtained in 1996 from the western slope of the Agulhas Bank off the coast of South Africa at 36°10.2′S and 19°28.2′E, at a water depth of 2488 m (Figures 1a and 1b). It was retrieved during the International Marine Global Change Studies Campaign II Namibia Angola Upwelling System and Indian Connection to Austral Atlantic Project cruise on board the *Marion Dufresne* [*Bertrand et al*., 1997].

We present results from the interval between 221.5 and 499.5 cm in the core, which according to the age model developed by *Martínez-Méndez et al*. [2008, 2010], spans the time interval 216 to 116 kyr. This age model is based on graphical correlation of the high-resolution benthic foraminiferal $\delta^{18}O$ record from core MD97-2120 located at 45°32′S and 174°57′E [*Pahnke et al*., 2003; *Pahnke and Zahn*, 2005] with the benthic $\delta^{18}O$ record from our core. As described by *Martínez-Méndez et al*. [2008], it is possible to compare the data on this age scale with the data from the spliced Cape Basin record of cores MD96-2081 and GeoB3603-2 [*Peeters et al*., 2004] due to the close structural fit of the benthic $\delta^{18}O$ of these records. Likewise, the use of a common benthic $\delta^{18}O$ chronology allows comparisons with previously published data from the Agulhas Plateau core MD02-2588 [*Marino et al*., 2013] as well as from the South Indian Gyre core MD96-2048 [*Caley et al*., 2011], for which benthic $\delta^{18}O$ analyses are reported [*Caley et al*., 2011; *Ziegler et al*., 2013] (Appendix A). The carbonate content of core MD96-2080 in our study interval ranges from 65 to 80% $CaCO_3$ [*Rau et al*., 2002].

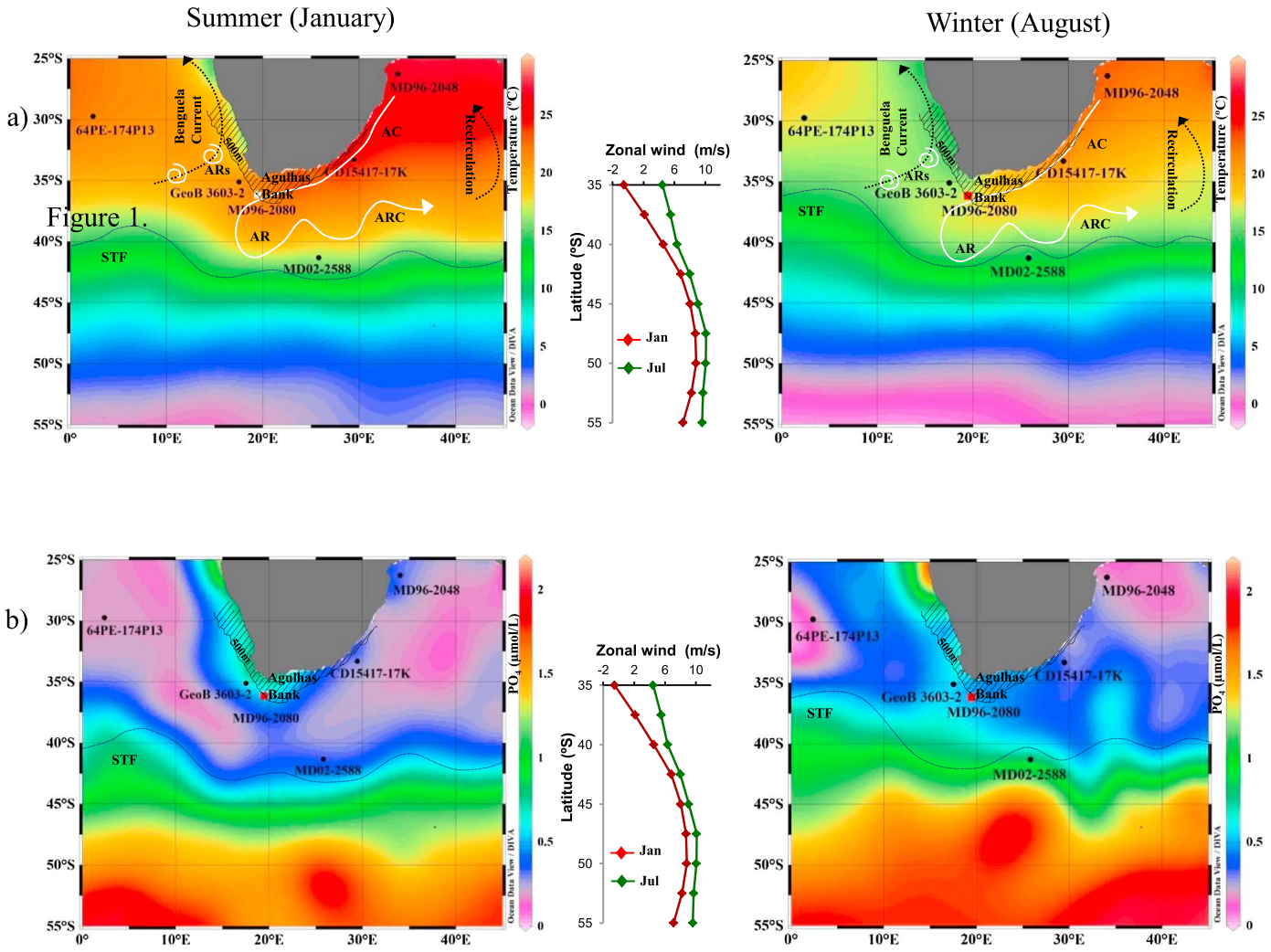


**Figure 1.** (a) Average monthly sea surface temperature map from January (summer) and August (winter) showing the overall picture of the Agulhas region. Location of core MD96-2080 (this study) in the Agulhas Bank slope as white and red squares in January and August, respectively. The white arrow indicates the path of Agulhas Current (AC) warm waters as it flows close and parallel to the southeastern African coast and retroflects at the southern Agulhas Bank (Agulhas Retroflection, AR), carrying with it most of the waters back to the Indian Ocean as the Agulhas Return Current (ARC). The part of the water reaching the South Atlantic through the formation of Agulhas rings (ARs) is carried northward by the Benguela Current. Recirculation of water in the ARC occurs in the southwest Indian Ocean subgyre. (b) Average monthly phosphate concentration map indicating the overall lower nutrient characteristics of waters in the Agulhas Bank slope during winter (August: decreased mixing) as compared to summer (January: increased mixing). Location of core MD96-2080 (this study) as red squares. The map also indicates the location of other cores mentioned in this study including MD02-2588 (Agulhas Bank), 64PE-174P13 (South Atlantic subtropical gyre), GeoB 3603-2 (Cape Basin), CD15417-17 K (southwest Indian Ocean), and MD96-2048 (South Indian subtropical gyre). The shaded area indicates the approximate location of the Agulhas Bank which follows the contour line of 500 m. The average position of the modern subtropical front (STF) has been reported to coincide with the 14°C isotherm at ~42°S [*Rau et al.*, 2002], and a graphical representation of its position is shown in the figures as a discontinuous line. Since recent studies have suggested that the STF may be discontinuous to the south of Africa [*Dencausse et al.*, 2011], the provided graphical representation is approximate. Average monthly zonal wind speed (westerlies >0 m/s) showing more intense westerlies during austral winter (July: green) as compared to austral summer (January: red). Zonal wind speed obtained from *Trenberth et al.* [1989]. Average monthly sea surface temperature and phosphate images compiled from World Ocean Atlas 09 using the Software Ocean Data View 4® (R. Schlitzer, Ocean data view, 2009, http://gcmd.nasa.gov/records/ODV_AWI.html).

The Agulhas Bank slope core lies in what is known as the Agulhas Corridor, a region of intersection between water masses from the South Atlantic, Indian, and Southern Oceans (Figure 1), each with distinct temperature, salinity, and nutrient characteristics [*Valentine et al.*, 1993]. From the Indian Ocean, warm, saline subtropical gyre waters are transported westward by the Agulhas Current (AC). Immediately south of the Agulhas Bank, the AC retroflects and turns back into the Indian Ocean as the Agulhas Return Current. Agulhas rings spin off the Agulhas retroflection and enter the Atlantic Ocean to form the Agulhas leakage [*Gordon et al.*, 1987; *Lutjeharms*, 2006; *Beal et al.*, 2011] (Figure 1a). Atlantic waters are brought to the region via the

South Atlantic Current and the southernmost extension of the Benguela upwelling system that advects cold subsurface waters over the western Agulhas Bank [*Chapman and Largier*, 1989; *Largier et al*., 1992; *Lutjeharms*, 2006]. Cold and fresh subantarctic surface waters reach the region by cross-frontal northward transport at the subtropical front (STF) [*de Ruijter et al*., 1999]. The STF, typically marked by a sea surface temperature (SST) isotherm of 14°C and located around 42°S, marks the ventilation location of subantarctic mode waters, which are the source of thermocline waters (depth 100–400 m) of the Agulhas Bank region [*Orsi et al*., 1995; *Belkin and Gordon*, 1996]. To date, most studies in the Agulhas Bank region have focused on the modern and past variations of hydrographical conditions and their relationship to Agulhas leakage, while productivity has received little attention.

### 2.2. Modern Primary Productivity Regime

Modern primary productivity along the southern margin of Africa has a strong seasonal cycle driven by alternations in the orientation of the wind field [*Jury*, 2011] (Figure 2), such that east flowing winds promote productivity, while west flowing winds decrease it. Although not as intense as the major upwelling systems on western continental boundaries (i.e., Benguela, Peru, Canary, and California), strong easterly trade winds along the Agulhas Bank region favor local upwelling events during austral summer (Figures 2c and 2d), when the South Atlantic anticyclone (SAA) shifts to the southeast and a low pressure system is set up over the southern part of the African continent [*Schumann et al*., 1995; *West et al*., 2004]. This upwelling shoals the nutricline (Figure 1b), although high surface radiation maintains surface thermal stratification (Figure 2f) and high SST (Figure 2e). Maximum chlorophyll *a* concentrations lag the maximum upwelling by 2 months as primary productivity peaks in autumn (March to May; Figure 2a), coincident with a shift to dominantly cyclonic wind vorticity/curl (cyclonic $<0$) (Figure 2b) still during a period of high wind stress (Figure 2d) [*Jury*, 2011]. Cyclonic wind curl has been invoked as causing a significant input of nutrients stimulating plankton production [*Rykaczewski and Checkley*, 2008]. On an interannual time scale, years of more intense January and February coastal upwelling result in higher chlorophyll *a* production 2 months later [*Jury*, 2011]. During El Niño years, unusually strong westerlies and/or their equatorward displacement causes an unusual summer northward migration of the SAA, which decreases the easterly trade winds, upwelling intensity and productivity in the region [*Schumann et al*., 1995].

In austral winter, the reduced solar heating in the Southern Hemisphere moves the low pressure associated with the Intertropical Convergence Zone to the Northern Hemisphere, shifting northward the easterly and southeasterly trade winds and forcing a northward migration of the SAA [*Schumann et al*., 1995]. The equatorward migration of polar fronts is accompanied by a more northward location and enhanced strength of the westerlies such that westerly winds predominate over the southern coast of Africa [*Esper et al*., 2004]. An increased winter influence of westerlies leads to downwelling, which strongly inhibits phytoplankton production from June to August on the Agulhas Bank (Figure 2a) [*Jury*, 2011]. In some years, the return of cyclonic wind curl in the spring leads to a brief minor peak in productivity in October, followed by a broad minimum with increasing stratification toward summer around November and December (Figure 2a) [*Jury*, 2011].

The generation of mesoscale eddies, which are related to the west flowing AC and are more frequent at increased leakage, may also influence productivity in the Agulhas Corridor. Although the AC water itself is poor in nutrients, periods of intense Agulhas leakage may promote a stronger mixing between deep and surface waters between the STF and the Cape of Good Hope as a consequence of eddy and baroclinic tide formation when the AC shoals against the Agulhas Bank during austral summers [*Cortese et al*., 2004], which enhance nutrient entrainment in the thermocline. Moreover, the formation of Agulhas rings in the retroflection area forms cold-core cyclonic eddies from the northward protrusion of the STF [*Lutjeharms and van Ballegooyen*, 1988], which locally stimulate nutrient entrainment to the surface and enhanced production. Agulhas rings are present over the site about 12% of the time in the modern ocean [*Rau et al*., 2002]. According to eddy-resolving models, Agulhas leakage has a maximum transport volume in February and March and minimum in July and August (Figure 2g) [*Reason et al*., 2003]. Since productivity peaks in autumn, a synchronous relationship between Agulhas leakage and eddy formation and productivity is not observed in the modern Agulhas system. Nonetheless, the Agulhas leakage may contribute to the extent of midsummer upwelling which is shown to influence the intensity of the autumn productivity peak 2 months later [*Jury*, 2011].

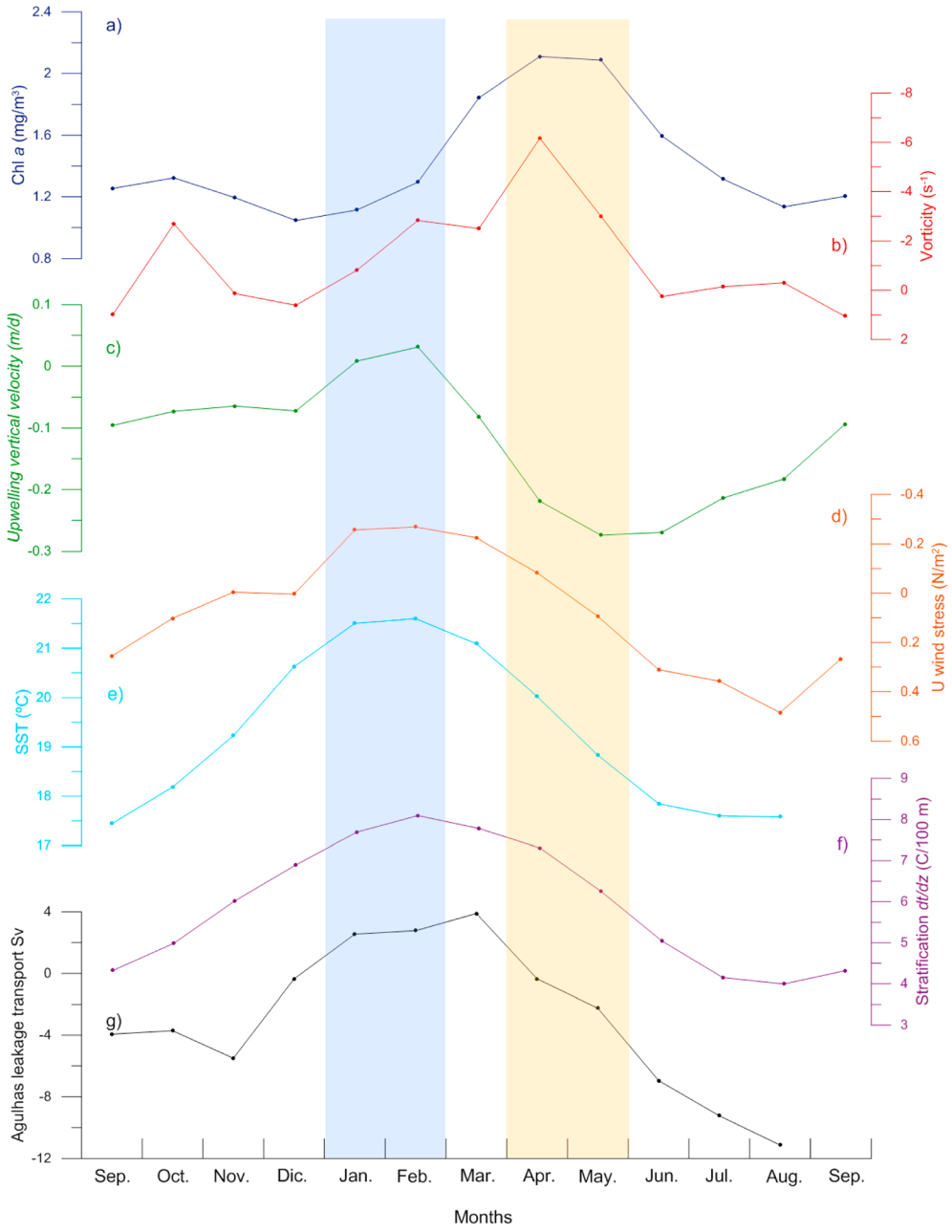


**Figure 2.** Monthly average water characteristics in the Agulhas Bank region during the period 1997 to 2007. (a) Mean chlorophyll *a* (Chl *a*) (mg/m$^3$) detected by Sea-viewing Wide Field-of-view Sensor and (b) wind vorticity (s$^{-1}$) shows that the peak in primary production and cyclonic wind curl ($<0$) takes place in autumn from March to May (orange shaded), i.e., 2 months after the highest peak in upwelling occurring during summer, especially from January to February (blue shaded). Highest peaks in (c) vertical velocity (upwelling $>0$) and (d) wind stress (N/m$^2$) (upwelling $U<0$) coincide with high local (e) sea surface temperature (SST) (°C) and increase in (f) stratification in the uppermost 100 m due to high summer insolation. (g) Modern Agulhas leakage transport (sverdrup) also peaks in summer during the maximum upwelling season and maximum SST. Chl *a*, wind vorticity, vertical velocity, wind stress, and stratification (0–100 m) from *Jury* [2011], SST from *Reynolds and Smith* [1994], and Agulhas leakage from *Reason et al.* [2003].

## 3. Analytical and Micropaleontological Methods

We present new measurements of Sr/Ca on the coccolith fraction of core MD96-2080 and coccolith assemblage data from the same core and conduct corrections of the temperature effect on Sr/Ca using the published records of Mg/Ca *G. bulloides*-derived SST for our same core site [*Martínez-Méndez et al.*, 2010], and

the effect of changing coccolith assemblages, to calculate the component of variation in Sr/Ca that is due to changes in productivity. These records are complemented by a record of water column stratification derived from coccolithophore assemblages.

### 3.1. Sr/Ca Analysis

For Sr/Ca analysis, ~250 mg of sediment from every sample was suspended in 2% ammonia solution to avoid carbonate dissolution and then sieved at 20 μm to obtain the coccolith-dominated <20 μm fraction. The coccolith fraction was cleaned as described by *Stoll and Ziveri* [2002] but without the oxidation step, since identical results were found in these sediments with and without oxidation. In brief, the method employs hydroxylamine HCl to reduce Fe and Mn oxyhydroxides that scavenge metals from seawater and that can contain noncarbonate Sr, and 2% ammonia solution to remove the Sr contained in the sediment clays by ion exchange with $NH_4^+$, followed by thorough rinsing of samples in ultrapure water. In order to dissolve coccoliths while minimizing the contribution of ions from noncarbonate phases, a weak buffered acid (0.1 M acetic acid/ammonium acetate buffer) was used to dissolve samples over 6 to 12 h.

Following carbonate dissolution, the acid was extracted and saved in acid-cleaned centrifuge tubes. A split of every sample was used to prepare dilutions to analyze Ca concentrations using a simultaneous dual inductively coupled plasma–atomic emission spectroscopy (ICP-AES) (Thermo ICAP DUO 6300) at the Universidad de Oviedo. Afterwards, samples were diluted to achieve homogeneous Ca concentrations. This minimizes matrix effects in the subsequent measurements of Sr/Ca on the same ICP-AES system, using radial detection of Sr421.5 nm and Ca315 nm. Calibration on ICP-AES was conducted using three standards with constant Ca concentrations and different Sr/Ca, which vary from 0.75 to 4 mmol/mol, following the intensity ratio method described by *de Villiers et al*. [2002]. Aliquots from those standards were uniformly diluted to obtain different Ca concentrations that match sample concentrations. The Sr/Ca analysis for coccoliths has a reproducibility of better than 0.02 mmol/mol based on in-house consistency standards. The Sr and Ca determinations on a total of 108 samples were performed.

### 3.2. Coccolithophorid Assemblages, CEX' Dissolution Index, and *Florisphaera Profunda* Index

Calcareous nannofossil assemblages from 149 samples, including all the samples in which Sr/Ca analysis was conducted, were identified by the preparation of rippled smear slides [*Bown and Young*, 1998] and their observation under a 1000X polarized microscope. For every sample, at least 300 specimens were identified and quantified. The counting error for *F. profunda* was smaller than ±5%.

Relative abundances were obtained for the most representative species of every assemblage, following the taxonomic concepts of *Young et al*. [2003]. Species' carbonate contribution from a total of 112 samples was obtained using the shape factors and equations proposed by *Young and Ziveri* [2000].

Dissolution variability at the site was evaluated using the *Calcidiscus leptoporus-Emiliania huxleyi + Gephyrocapsa ericsonii* Dissolution Index (CEX'), which is obtained from the equation: CEX' = *Emiliana huxleyi + Gephyrocapsa ericsonii/E. huxleyi + G. ericsonii + Calcidiscus leptoporus* [*Boeckel and Baumann*, 2004]. Because the large placoliths of *C. leptoporus* are more resistant to dissolution, increased dissolution lowers the CEX'. While these taxa are generally all favored under more productive conditions, shifts in the photic zone production of small fragile coccoliths relative to the more resistant *C. leptoporus* (or vice versa) can also affect the CEX', independent of dissolution.

Water column stratification was evaluated by calculating the *F. profunda* index as follows: *F. profunda*/(*F. profunda* + *E. huxleyi*). Since *F. profunda* is the main deep photic zone species in our samples, low values for this index indicate water column mixing conditions, while values close to 1 imply a deeper nutricline/thermocline and greater stratification [*Beaufort*, 1997; *Beaufort et al*., 2001].

### 3.3. Stable Isotope Analysis

The <20 μm cleaned coccolith fraction was also analyzed for oxygen and carbon isotopic composition for a total of 62 samples. Coccolith $\delta^{18}O$ values were compared to those of *G. bulloides* [*Martínez-Méndez et al*., 2010] to verify, for the studied location and time interval, the similarity of their seasonality and habitat depth which has been shown elsewhere in sediment trap studies [*Stoll et al*., 2007d]. Because coccoliths of different sizes exhibit different stable isotopic vital effects [*Dudley and Goodney*, 1979; *Ziveri et al*., 2003; *Bolton and Stoll*, 2013], we selected mainly samples, where the contribution of carbonate by large

coccoliths was in the range of 35 to 60% and for which published $\delta^{18}O$ data were available from foraminifers *Globigerina bulloides* and *Globigerinoides ruber* [*Martínez-Méndez et al*., 2010; *Marino et al*., 2013]. The difference between $\delta^{13}C$ from coccoliths and *G. bulloides* provides information about the magnitude of carbon isotopic fractionation in the coccoliths, assuming *G. bulloides* $\delta^{13}C$ records $\delta^{13}C$ variations of seawater-dissolved inorganic carbon (DIC).

Coccolith $\delta^{18}O$ and $\delta^{13}C$ were measured on a Nu Perspective dual-inlet isotope ratio mass spectrometer connected to a NuCarb carbonate preparation system, with an analytical precision of 0.06‰ for $\delta^{18}O$ and 0.05‰ for $\delta^{13}C$ (1σ), at the University of Oviedo.

*G. bulloides* $\delta^{13}C$ (250–315 μm size fraction) was obtained from the analysis of 20 individuals using a ThermoFinnigan MAT 252 mass spectrometer linked online to a single acid bath CarboKiel-II carbonate preparation device at the University of Barcelona as detailed by *Martínez-Méndez et al*. [2010], where the $\delta^{18}O$ results were first reported. External precision was better than ±0.06‰ (1σ). Both coccolith and *G. bulloides* isotope values are reported relative to the Vienna Peedee belemnite (VPDB) via calibration to the National Bureau of Standards 19 carbonate standard.

## 4. Deriving the Productivity Record From the Agulhas Bank Slope

### 4.1. Results of Coccolith Sr/Ca and Assemblages

The carbonate analyzed in the coccolith size fraction was composed of *C. leptoporus*, *Helicosphaera carteri*, *Gephyrocapsa oceanica*, *Coccolithus braarudii*, and *Gephyrocapsa muellerei*, with minor contributions by other species. The relative contributions of these species were relatively stable over the studied period. A slightly higher relative carbonate contribution of *C. leptoporus* was recorded during the late glacial and marine isotope stage (MIS) 5, and relatively higher contributions of *G. muellerei* were observed during part of the glacial (Figure 3a). The CEX' averaged 0.72 and ranged from 0.6 to 0.9 in most of the studied interval, confirming an overall good preservation of the sediments and minimal alteration of the assemblage due to dissolution (Figure 3g).

The Sr/Ca ratio results ranged from 1.72 to 2.24 mmol/mol, showing low-frequency variability. Minima in Sr/Ca were observed at ~187 and ~141 ka, while high Sr/Ca values characterized the earliest part of MIS 7, the midglacial, MIS 6-MIS 5 transition, and the highest values were recorded in the MIS 5 interglacial (Figure 3c).

Isolation of the Sr/Ca productivity signal from measured Sr/Ca ratios requires constraining temperature effects, assessing the assemblage influence and dissolution variability effect on coccolith Sr/Ca trends, as we detail in the subsequent section.

### 4.2. Extraction of Productivity Component From Measured Sr/Ca Ratios

#### 4.2.1. Temperature Correction

To remove from the Sr/Ca time series the positive linear dependence of Sr/Ca on temperature, we used equations derived from the observed dependence of Sr/Ca on temperature in cultures [*Stoll et al*., 2002a; *Müller et al*., 2014], together with an independent temperature (*T* °C) record from our core. Carbonate in the coccolith fraction of MD96-2080 was dominated by *C. leptoporus*, *H. carteri*, *G. oceanica*, and *C. braarudii* with average contributions of 21.8%, 18.6%, 16.8%, and 10.2%, respectively (Figure 3a). These species exhibit similar slopes of Sr/Ca versus temperature, despite differences in absolute ratios among species, and were combined to generate a single temperature regression ($Sr/Ca = 0.0501T + 1.7053$) as detailed in the supporting information (Appendix B).

The SST history of core MD96-2080 derived from *G. bulloides* Mg/Ca [*Martínez-Méndez et al*., 2010] (Figure 3b) was chosen for the temperature correction for several reasons. First of all, the season of maximum export of this planktic foraminifer closely matches that of coccolithophores in sediment trap studies [*Stoll et al*., 2007d]. *G. bulloides* is preferentially produced in the mixed layer in cool and high-nutrient waters [*Ganssen and Kroon*, 2000; *Chapman*, 2010] in periods of high primary productivity, especially during upwelling events [*Nianqiao et al*., 2001; *Mortyn and Charles*, 2003; *Reichart and Brinkhuis*, 2003]. For MD96-2080, Mg/Ca SST and $\delta^{18}O$ records are available for planktic foraminiferal species *G. ruber* [*Marino et al*., 2013] as well as *G. bulloides* [*Martínez-Méndez et al*., 2010]. However, these two species exhibit different amplitudes in $\delta^{18}O$ change across the major transitions. The $\delta^{18}O$ from the coccolith fraction and *G. bulloides* showed similar magnitudes and

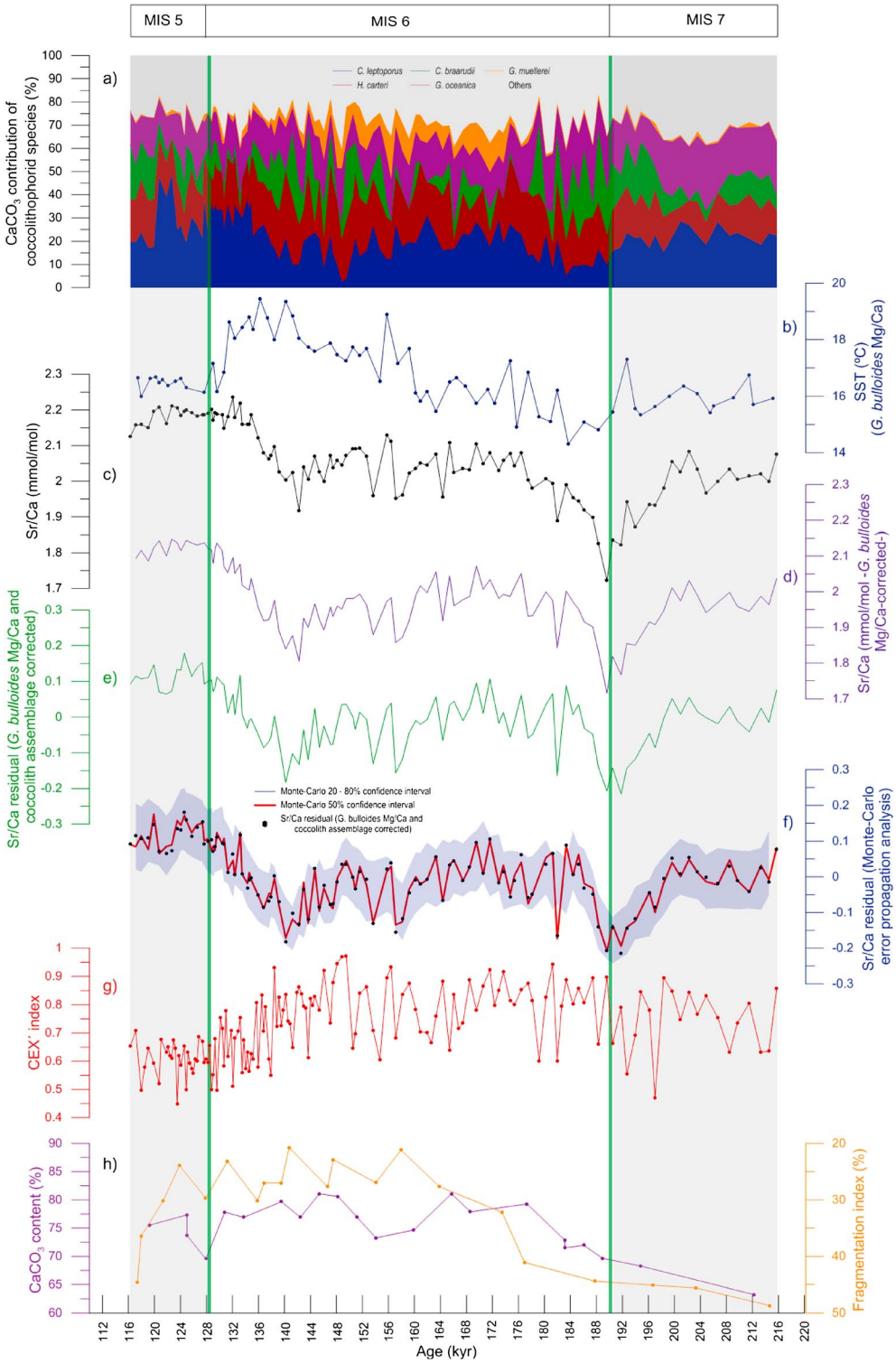


**Figure 3**

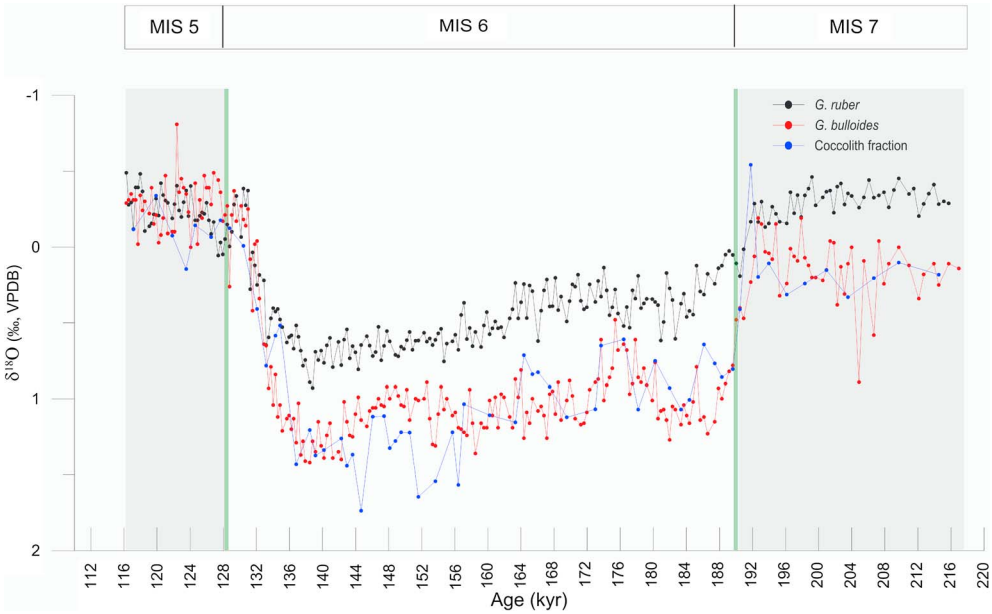


**Figure 4.** The $\delta^{18}O$ (‰, VPDB) records from the <20 μm coccolith fraction (this study; blue), the planktic foraminifer *G. bulloides* [*Martínez-Méndez et al*., 2010] (red) and from the planktic foraminifer *G. ruber* (sensu lato, white morphotype) [*Marino et al*., 2013] (black) from core MD96-2080 in the Agulhas Bank. All are plotted on the same scale to illustrate the similar magnitude of $\delta^{18}O$ change in the coccolith fraction and *G. bulloides*. Gray shaded areas and green lines as in Figure 3.

trends, and $\delta^{18}O$ were on average more positive than those from *G. ruber* [*Marino et al*., 2013], especially during the glacial MIS 6. One interpretation is that the subtropical species *G. ruber* was produced only at times when water temperatures were above its comparatively warm temperature tolerance. In contrast, *G. bulloides*, which tolerates cooler temperatures, is able to record the more extreme cold conditions during the glacial. The similar amplitude, structure, and timing of $\delta^{18}O$ transitions in the *G. bulloides* [*Martínez-Méndez et al*., 2010] and coccolith records (Figure 4) further support the hypothesis that both experienced similar growth and calcification temperatures during the studied interval, likely because of similar seasonality and depth of production. This confirms that for the studied interval, the *G. bulloides* record is thus the most appropriate for correcting temperature effects on coccolith Sr/Ca. The agreement between coccolith and *G. bulloides* $\delta^{18}O$ does not seem to be affected by differences in relative carbonate contribution of large (*C. leptoporus* + *H. carteri*) versus small coccoliths in the cocccolith fraction ($r = -0.093$; $p = 0.473$; $n = 62$).

**Figure 3.** Records from core MD96-2080 for the interval 116.3–215.7 kyr. (a) Relative calcite contribution (% $CaCO_3$) of the dominant carbonate contributors (*Calcidiscus leptoporus*, *Helicosphaera carteri*, *Coccolithus braarudii*, *Gephyrocapsa oceanica*, and *Gephyrocapsa muellerei*) in the coccolith fraction. (b) Mg/Ca-derived SST record from the planktic foraminifer *Globigerina bulloides* from core MD96-2080 [*Martínez-Méndez et al*., 2010] used here to correct the temperature effect on measured Sr/Ca ratios. (c) Measured Sr/Ca in coccolith fraction (<20 μm). (d) Coccolith Sr/Ca obtained after temperature correction using *G. bulloides* Mg/Ca-derived SST [*Martínez-Méndez et al*., 2010] and the combined temperature dependencies of the four main carbonate contributors of the coccolith assemblage (*C. leptoporus*, *H. carteri*, *G. oceanica*, and *C. braarudii*) normalized to 15°C. (e) Coccolith Sr/Ca productivity obtained after temperature correction as in Figure 3d and removal of the linear dependence of temperature-corrected Sr/Ca on coccolith assemblage ((Sr/Ca = 0.0036 × (% $CaCO_3$ from *C. leptoporus* and *H. carteri*) + 1.844) from the series. (f) Coccolith Sr/Ca productivity after conducting a Monte Carlo simulation methodology to show the propagated errors of the temperature and assemblage-corrected productivity record in Figure 3e. Analytical errors of temperature and Sr/Ca measurements, quantification of species and uncertainties of the temperature, and assemblage dependencies were included in the Monte Carlo analysis. Black data points illustrate direct application of the temperature and assemblage correction to Sr/Ca measurements with no error propagation. The blue shaded area shows the 20–80% confidence intervals and are plotted as three-point running average to highlight the long-term productivity trends we interpret, as opposed to the 50% confidence interval (red line), which shows the high-frequency variability of the productivity record and therefore may fall beyond 20–80% smoothed confidence intervals. (g) CEX′ (*E. huxleyi* + *G. ericsonii*/*E. huxleyi* + *G. ericsonii* + *C. leptoporus*). (h) $CaCO_3$ content (%) (purple) and planktic foraminifera fragmentation index (%) (yellow) of core MD96-2080 from *Rau et al*. [2002] as dissolution proxies. Gray shaded areas mark the interglacial stages MIS 7 and MIS 5, and green vertical lines mark the boundaries between stages.

The *G. bulloides* SST history displays a progressive warming during the glacial MIS 6 that culminates during Termination II (TII), immediately before the onset of MIS 5 (Figure 3b). The early warming likely reflects changes in the regional surface ocean circulation and vertical water column structure as glacial conditions intensified during MIS 6 [*Martínez-Méndez et al*., 2010]. The maximum temperature during TII coincides with increased abundance of tropical-subtropical foraminifera in the Cape Basin [*Peeters et al*., 2004] and maximum SST from *G. ruber* Mg/Ca [*Marino et al*., 2013] and likely reflects the enhanced influx of warmer waters from the Indian Ocean.

When we correct the Sr/Ca record for the component of variation attributable to temperature as described above, the temperature-corrected Sr/Ca variation that can be attributed to productivity is similar to the uncorrected Sr/Ca record (Figures 3d and 3c, respectively). This shows that the observed range of temperature variation contributed only a small component of variability to the Sr/Ca record (Figure 3d).

#### 4.2.2. Assemblage Correction

In addition to temperature, we have also evaluated the effect of variations in the coccolithophore species contributing to the assemblage composition of the coccolith fraction. Higher Sr/Ca have been reported for the medium to large coccolith size fraction (5–15 μm) compared to the small fraction (<5 μm) for some surface sediments from the equatorial and South Atlantic [*Fink et al*., 2010]. Where coccoliths of a single genera have been isolated from sediment traps and sediments and analyzed for Sr/Ca via ion probe, in some cases, the larger coccoliths *C. leptoporus* and *H. carteri* had Sr/Ca ratios higher than other species [*Stoll et al*., 2007a]. If the *C. leptoporus* and *H. carteri* of the Agulhas Bank slope core were likewise significantly higher in Sr, then, changes in their abundance relative to other species might introduce nonproductivity-related variations in the Sr/Ca of the coccolith fraction. Because the difference between these species and others is variable, presumably depending on the environmental and ecological conditions of the site, we cannot apply an independent correction factor as we have done for temperature. Instead, we take a conservative approach and assume that all of the covariation between temperature-corrected Sr/Ca and the carbonate contribution of *C. leptoporus* and *H. carteri* ($r = 0.38$; $p < 0.01$; $n = 108$; Appendix C), is due to the effect of the possibly higher Sr content of these species. In reality, this correlation could also arise, in part, if these species became more abundant during highly productive times. Therefore, we may overestimate the species' effect by using this approach. The resulting residuals from this correlation indicate that variance in Sr/Ca is limited to the productivity signal and therefore not driven by changes in the assemblage.

A Monte Carlo approach was used to analyze the data and compute the confidence intervals of the results. Each of the 108 data points is simulated with 100 Monte Carlo histories which yield over 10,000 cases. The propagated error calculated considering measurement uncertainties of temperature (with $\sigma = 0.3$°C), Sr concentration (with $\sigma = 0.01$ mmol/mol), and species quantification (with $\sigma = 3\%$) were simulated, together with the uncertainty resulting from the regression of temperature versus Sr ($\sigma = 0.12$ mmol/mol). The largest source of statistical variability was the correction of the Sr with temperature. After each history was factored for temperature and various measurement errors, the residuals of the correlation with species' assemblage were examined. The Monte Carlo simulation permits the 20%, 50%, and 80% confidence intervals to be calculated and compared to the results without error propagation (Figure 3f; Appendix D).

### 4.3. Is There a Relationship With Dissolution or Carbon Isotope Fractionation in Coccoliths?

While the chemical heterogeneity in planktic foraminifera can give rise to a strong influence of dissolution on some elemental ratios [*Brown and Elderfield*, 1996], such effects are not expected in the more homogenous calcite of coccoliths [*Stoll et al*., 2007a]. Although dissolution indices from foraminiferal fragmentation and % $CaCO_3$ appear slightly more sensitive than coccolith dissolution indicators (CEX') in core MD96-2080 (Figures 3h and 3g, respectively), none of these dissolution proxies exhibited trends similar to the Sr/Ca record (Figure 3c). Indices of planktic foraminiferal fragmentation index from our core broadly follow the % $CaCO_3$ [*Rau et al*., 2002] (Figure 3h), suggesting a similar forcing by dissolution and minimal bias by winnowing and terrigenous dilution. The progressive decrease in fragmentation and increase in % $CaCO_3$ from ~216 to 176 kyr contrasts with the more stable coccolith dissolution indicator in the CEX' (Figure 3g). We suggest that this difference reflects the lower susceptibility of coccoliths to dissolution compared to foraminifera [*Chiu and Broecker*, 2008]. Significantly, there is no evidence for an unusual peak of high or low dissolution in any of these indicators during the oldest Sr/Ca excursion between 189.6 and 191.8 kyr. South of the Agulhas Bank, in the deepest waters of the Cape Basin (~4600 m), which are bathed by Circumpolar Deep

Water (CDW), the MIS 7-MIS 6 boundary is recognized as a strong event of deep-sea carbonate dissolution [*Hodell et al*., 2003]. While this event coincides with a coccolith Sr/Ca productivity minimum, there is no manifestation of dissolution in any of the carbonate preservation indices in the shallower Agulhas Bank slope location (2488 m) currently bathed by North Atlantic Deep Water. It is possible that the changes in oceanic or atmospheric circulation of the CDW formation regions, which drove this carbonate dissolution event, also contributed to a shift in productivity regime in the Agulhas Bank region.

The more recent minimum in coccolith Sr/Ca productivity (between ~142.3 and 140.2 kyr) coincides with relatively high CEX′ values and a long and stable period of low foraminiferal fragmentation and high % $CaCO_3$. Conversely, the recovery from this Sr/Ca minimum corresponds with the onset of descending CEX′ values. Consequently, the weak negative correlation between the CEX′ and measured Sr/Ca ($r = -0.45$; $p < 0.01$; $n = 108$) in the overall record was driven by the low CEX′ values from ~140 to 115 kyr, which correspond to increasing Sr/Ca. Because the % $CaCO_3$ and foraminiferal fragmentation indices appear to be more sensitive to dissolution compared to the CEX′, this depression of CEX′ values during a period of stable high % $CaCO_3$ and low foraminiferal fragmentation may not reflect a change in dissolution intensity. Rather, it may have been driven by higher relative production of *C. leptoporus* in the photic zone, which may be associated with the higher productivity reflected in Sr/Ca productivity. In conclusion, despite some shoaling of the lysocline in this region during glacial times [*Bickert and Wefer*, 1996; *Martínez-Méndez et al*., 2008], the evidence discussed above makes it unlikely that changing dissolution has driven the trends in the observed Sr/Ca ratios.

Some culture studies have recently suggested that, in addition to temperature and growth rate, coccolith Sr/Ca may also be influenced by $CO_2$ in seawater [*Müller et al*., 2014]. The pattern of corrected Sr/Ca variation in the Agulhas Bank slope does not appear to be strongly driven by atmospheric $CO_2$ over the studied interval. Recent models show that the carbon isotopic fractionation in coccolith calcite (defined as $\varepsilon_{coccolith}$) may track adaptations developed by coccoliths in response to varying $CO_2$ [*Bolton and Stoll*, 2013]. We examine $\varepsilon_{coccolith}$ in our record to evaluate if such adaptations might have influenced coccolith Sr/Ca in our studied interval. We calculate an apparent $\varepsilon_{coccolith}$ from the difference between coccolith $\delta^{13}C$ and *G. bulloides* $\delta^{13}C$, assuming that *G. bulloides* records the temporal variation in $\delta^{13}C$ of seawater DIC, albeit potentially with a constant offset. The $\delta^{13}C$ of coccoliths was higher than that of *G. bulloides* by an average of 1.45‰. The difference between $\delta^{13}C$ of the coccolith fraction and *G. bulloides* was not correlated with the carbonate contribution from large coccoliths (*C. leptoporus* + *H. carteri*) ($r = 0.069$; $p = 0.596$; $n = 62$), showing that assemblage variations were not responsible for temporal variation in $\varepsilon_{coccolith}$. The $\varepsilon_{coccolith}$ has varied during the penultimate glacial cycle and was found to be on average larger during the glacial period than during MIS 7 (Appendix E). The low seawater $pCO_2$ and/or the high productivity of the glacial interval appear to increase the magnitude of $\varepsilon_{coccolith}$. Given that the temporal variation in the coccolith Sr/Ca productivity record does not correspond with periods of anomalous $\varepsilon_{coccolith}$, we conclude that glacial-interglacial $CO_2$ variations did not significantly affect the coccolith Sr/Ca trend.

### 4.4. Productivity History on the Agulhas Corridor

The resulting Sr/Ca productivity record shows significant low-frequency variability (Figure 3d). The productivity declined over the transition between MIS 7 and MIS 6, with a minimum reached between ~189.6 and 191.8 kyr, followed by a rapid recovery. Throughout the rest of MIS 6, the productivity remained relatively stable and high until 144.7 ka when it began to decline, reaching a minimum between ~142.3 and 140.2 kyr. During the late glacial, the productivity increased steeply, reaching maximum values during TII and subsequently started to decrease slightly during early MIS 5.

This pattern of productivity variation is also evident in other indicators of productivity and nutrient availability in the Agulhas Corridor, including our new data on coccolith assemblages from this site (*F. profunda* index), as well planktic foraminiferal assemblage data published previously from nearby locations [*Peeters et al*., 2004] (Figure 5). Periods of strong upper water column stratification and oligotrophic conditions lead to increasing dominance of lower photic zone taxa such as *F. profunda* [*Beaufort*, 1997; *Beaufort et al*., 2001; *Grelaud et al*., 2012], which can be expressed as the *F. profunda* index which ranges from 0 for a highly mixed water column to 1 for a highly stratified one. In the Agulhas Bank slope, the *F. profunda* index suggests a deeper thermocline/nutricline between stage 7 and stage 6, with highest abundance of *F. profunda* and highest stratification at ~188 ka. No or only low-intensity mixing events were

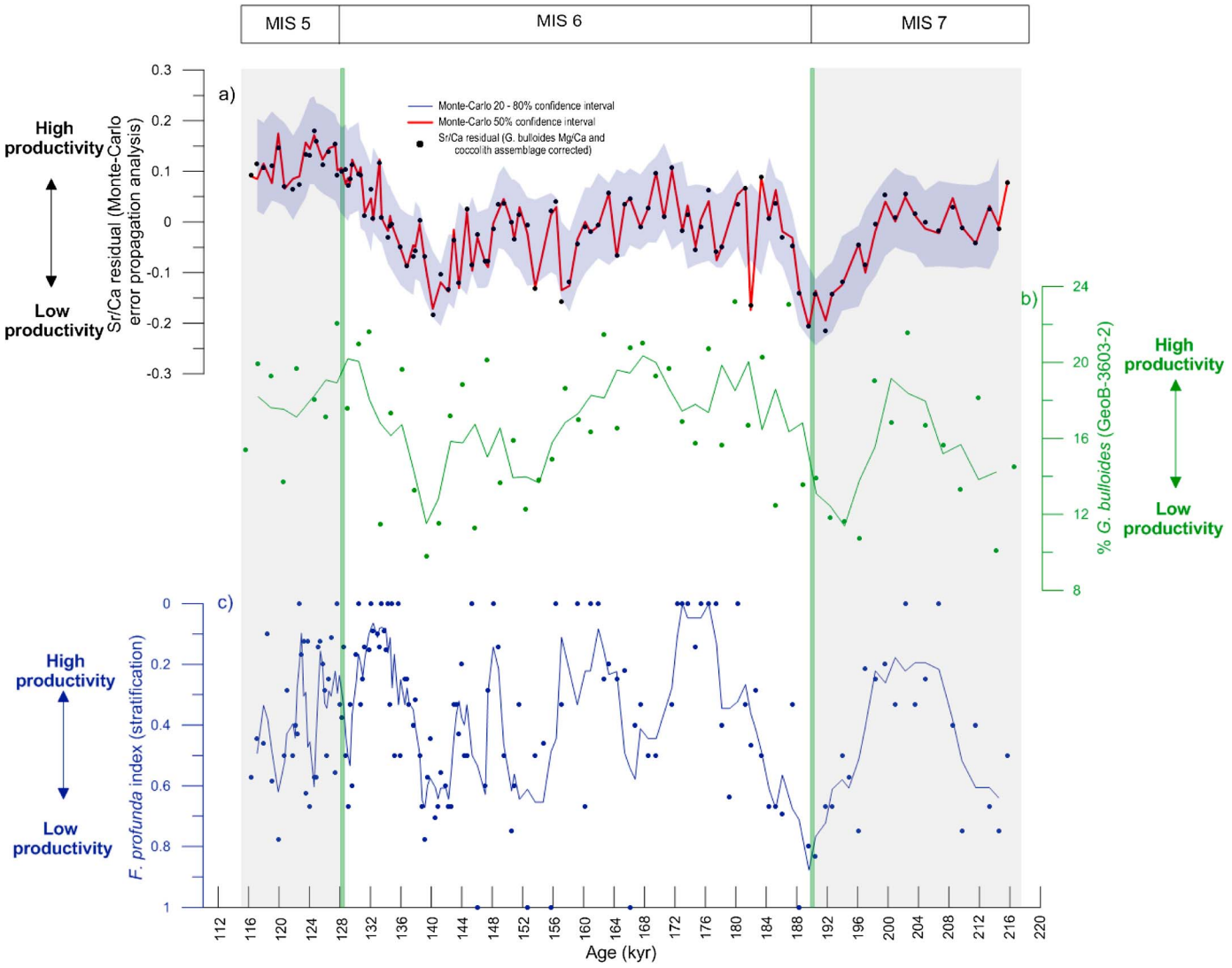


**Figure 5.** Productivity indices in the Agulhas Bank. (a) Coccolith Sr/Ca productivity record from core MD96-2080 (this study), as illustrated in Figure 3f. (b) Relative abundance of planktic foraminifera *G. bulloides* from core GeoB-3603-2 in Cape Basin [*Peeters et al.*, 2004]. (c) *F. profunda* index (*F. profunda*/(*F. profunda* + *E. huxleyi*)) from core MD96-2080 (this study). Three-point running average shown for Figure 5b (solid green) and Figure 5c (solid blue) to evidence trends clearer due to high variability in the data. Gray shaded areas and green lines as in Figure 3.

indicated by the *F. profunda* index until around 181 ka. Average *F. profunda* abundances are low through most of the glacial (glacial average abundance 0.369 ± 0.280), which suggests relatively high but variable subsurface nutrient enrichment. Although cold temperatures may contribute to the exclusion of this species, the period of coldest temperatures recorded by *G. bulloides* Mg/Ca (~188–181 kyr) did not result in exclusion of *F. profunda* but instead coincided with high relative abundances. Thus, we infer that low abundances of *F. profunda* during subsequent and slightly warmer parts of MIS 6 are indicative of strong water column mixing and not temperature exclusion. An additional increase in stratification occurred in the midlate glacial MIS 6. Lastly, a more variable and steep increase in stratification is observed at the end of the studied period (Figure 5c). A similar overall productivity pattern compared to coccolith Sr/Ca productivity was observed in the *F. profunda* index, although slightly higher productivities are generally inferred from a complete overturning in periods in which high productivities are indicated by both proxies (e.g., during late MIS 7, MIS 6 from ~178 to 172 kyr, from ~164 to 157 kyr, around 148 ka, and late MIS 6) (Figures 5a and 5c). Overall, the record suggests that periods of high productivity indicated by Sr/Ca were periods of enhanced mixing of nutrients into the euphotic zone, whereas periods of low productivity indicated by Sr/Ca were periods of water column stratification.

Similar minima in productivity at 191 and 140 ka are suggested by minima in the abundance of *G. bulloides*, a planktic foraminifer that is widely used as an indicator of upwelling, nutrient-rich areas, and paleoproductivity [*Nianqiao et al*., 2001; *Mortyn and Charles*, 2003; *Reichart and Brinkhuis*, 2003]. This species dwells in cool and nutrient-rich waters in the surface mixed layer above the thermocline [*Ganssen and Kroon*, 2000; *Chapman*, 2010] and is abundant in areas characterized by pronounced seasonal upwelling, where the high phytoplankton concentration attracts abundant prey [*Salgueiro et al*., 2008; *Wilke et al*., 2009]. The relative abundance of *G. bulloides* from core GeoB-3603-2 in Cape Basin [*Peeters et al*., 2004], which is ~207 km northwest of MD96-2080, shows similar trends to the coccolith Sr/Ca productivity record over the studied time interval (Figures 5a and 5b). Decreasing productivity values shown by both proxies were observed from late MIS 7, remaining relatively low at the transition between MIS 7 and MIS 6, when the lowest coccolith Sr/Ca productivity was found. A subsequent increasing trend was recorded, with high productivities during the early glacial, which were maintained until midlate MIS 6. A second decreasing trend that started at ~149.5 ka became steep at ~144.7 ka and reached the lowest values at ~142.3, and 140.2 ka was observed in the Sr/Ca productivity proxy. A more variable, though still decreasing trend, is also evidenced with the relative abundance of *G. bulloides* during this time interval. Finally, during late glacial, MIS 6-MIS 5 transition and early interglacial, both proxies show a steep increase of productivity and subsequent decrease (Figures 5a and 5b). The good agreement between the upwelling (% *G. bulloides*) and paleoproductivity (coccolith Sr/Ca) proxies may imply that even though the Cape Basin core GeoB-3603-2 was located farther north of core MD96-2080, climatic and oceanographic factors controlling productivity may have exerted a similar influence in the whole Agulhas Corridor.

## 5. Discussion

### 5.1. Productivity Response to Southern Hemisphere Midlatitude Westerlies

#### 5.1.1. Productivity on the Agulhas Bank Slope Decreases Strongly During Extreme Southern Ocean Cold Events

The timing of the three productivity minima observed in our coccolith Sr/Ca record from the Agulhas Bank slope coincides exactly with peaks in ice-rafted detritus (IRD) from core MD02-2588 on the Agulhas Plateau south of our core site [*Marino et al*., 2013] (periods A in Figure 6). The presence of IRD indicates extreme cold phases during which polar waters were advected to the Agulhas Plateau, which may reflect a large expansion (i.e., equatorward displacement) of the subantarctic frontal system [*Marino et al*., 2013; *Simon et al*., 2013]. These extreme cold events (Figure 6d) and associated low productivities (Figure 6b) appear to be conditioned by obliquity minima (Figure 6a). Cross-spectral analysis confirms that obliquity and IRD concentration in core MD02-2588 [*Marino et al*., 2013; *Simon et al*., 2013] are coherent at the 95% confidence interval in the obliquity (41 kyr) band (Appendix F). More subtle changes in response to reorganizations of the subantarctic frontal system, with strong glacial-interglacial (100 kyr) pacing, have been recorded by other faunal and temperature reconstructions at other more northward core locations [*Peeters et al*., 2004].

Recent atmospheric modeling studies indicate that low SSTs over the southern extratropics enhance westerly flow off the southwest coast of Africa [*Sime et al*., 2013]. This northward expansion of the influence of the westerlies would be consistent with a northward migration of oceanic fronts, since the location of the westerlies is believed to follow the frontal system (*Beal et al*. [2011], although see *Kohfeld et al*. [2013] for caveats). The cold events reflected in the IRD pulses at the Agulhas Plateau also correspond with unusually cold summer SST, as recorded by the summer growing *G. bulloides* on the Agulhas Plateau [*Marino et al*., 2013]. We suggest that a more northward extent of the westerly wind belt and STF decreased productivity by maintaining the westerlies in an unusually northward location through the austral summers. At the latitude of the Agulhas Bank slope, these westerlies would block the easterly trade wind circulation which promotes strong water column mixing and production.

#### 5.1.2. Further Evidence for Westerly and Frontal Variability in the South Indian Ocean

A link between productivity and changes in the westerly wind system is supported by coeval salinity changes in the South Indian subtropical gyre that likewise respond sensitively to the poleward contraction of westerlies and concomitant migration of the regional fronts. In the South Indian subtropical gyre (core MD96-2048), in the AC source region, over the last 800 kyr, periods of low obliquity are marked by fresher (and cooler) Indian Ocean waters [*Caley et al*., 2011]. Within the time period studied at the Agulhas Bank slope, the resolution of the South Indian subtropical gyre record is not sufficient for these cycles to be clearly defined (Figure 6c). However, the general correlation suggests that low salinity would coincide with lower Agulhas Bank slope productivity during

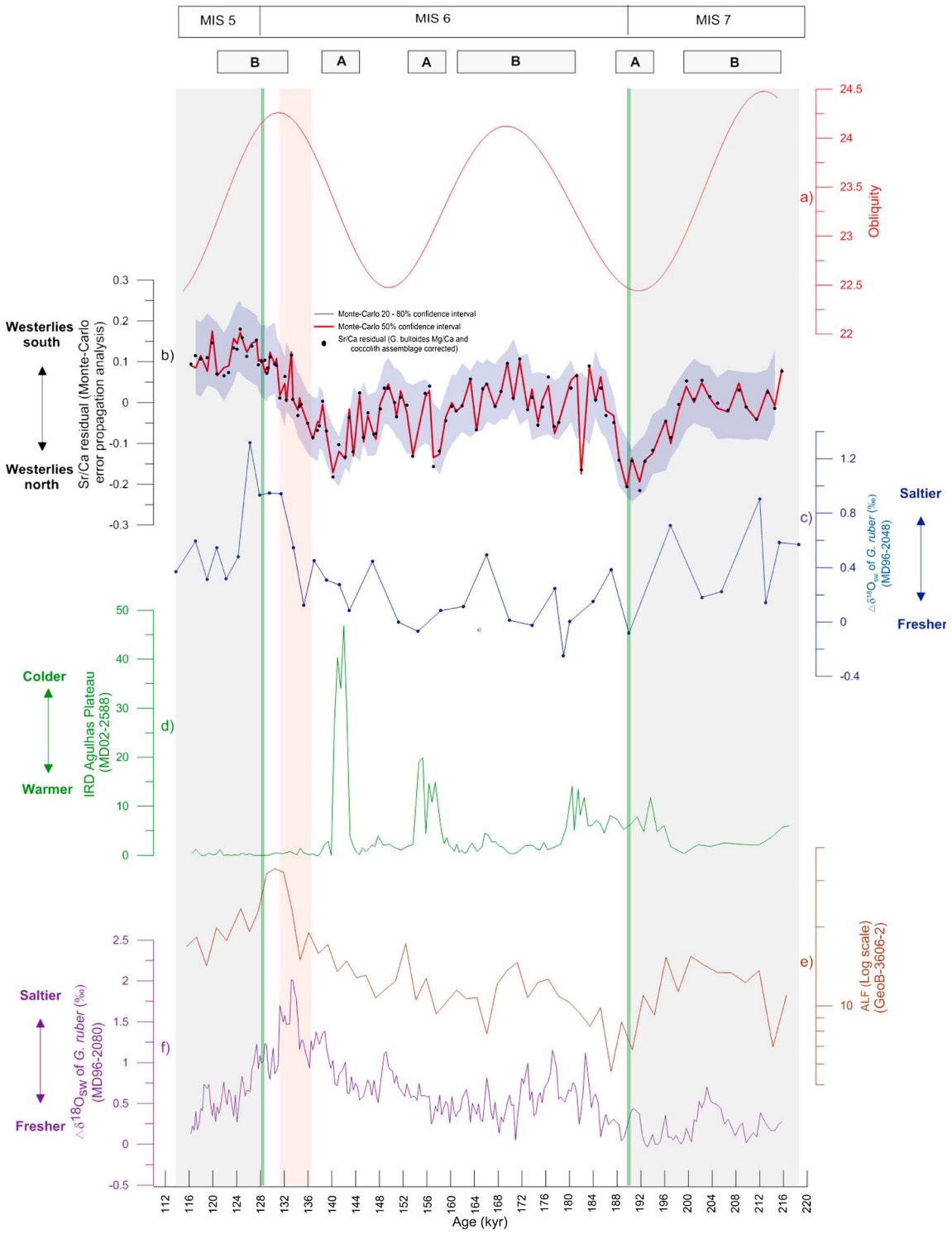


**Figure 6.** Records of surface ocean variability in the Agulhas Bank slope, Cape Basin, Agulhas Plateau, and South Indian subtropical gyre. (a) Obliquity. (b) Coccolith Sr/Ca productivity record from core MD96-2080 (this study) as illustrated in Figure 3f. (c) $\Delta\delta^{18}O_{sw}$ (‰) derived from paired $\delta^{18}$O-Mg/Ca analyses in *Globigerinoides ruber* as a proxy of sea surface salinity (SSS) changes in the South Indian subtropical gyre from core MD96-2048 [*Caley et al.*, 2011]. (d) Ice-rafted detritus (IRD) from core MD02-2588 in the Agulhas Plateau [*Marino et al.*, 2013]. (e) Abundance of tropical-subtropical foraminifera (ALF) from Cape Basin [*Peeters et al.*, 2004] plotted on a logarithmic scale. (f) $\Delta\delta^{18}O_{sw}$ (‰) derived from paired $\delta^{18}$O-Mg/Ca analyses in *G. ruber* (‰) as a proxy SSS in the Agulhas Bank from core MD96-2080 [*Marino et al.*, 2013]. Red shading highlights steep increase in ALF (Figure 6e) and SSS from core MD96-2080 (Figure 6f) coincident with the sharp increase in productivity before TII. A and B indicate periods of productivity minima/high productivities during low/high obliquity, respectively. Gray shaded areas and green lines as in Figure 3.

low obliquity. According to recent models, salinity in the AC source region is controlled by variability in the Agulhas Return Current recirculation due to meridional shifts of fronts and westerlies [*Simon et al*., 2013]. A strengthening or equatorward displacement of the westerlies intensifies the southwest Indian Ocean subgyre, allowing colder/freshwaters from the south to be introduced into the Agulhas Return Current [*Durgadoo et al*., 2013; *Simon et al*., 2013]. Therefore, our hypothesis that decreased productivity results from northward expansion of the westerlies and STF during low obliquity is coherent with this mechanism for a cooler/fresher South Indian subtropical gyre [*Caley et al*., 2011].

#### 5.1.3. Manifestation of Westerlies and Frontal Changes in Hydrological Characteristics of the Agulhas Corridor and South Atlantic Gyre

The salinity variation caused by westerlies and STF movement reported for the southwest Indian Ocean [*Simon et al*., 2013] also appears to be manifested in the Agulhas Corridor. A greater subtropical character (higher temperature and salinity) of waters in the southwest Indian Ocean (core CD154 17–17 K) has been shown to correlate with warmer/saltier waters in the Agulhas Corridor over the last 100 kyr [*Simon et al*., 2013]. This could occur because the southwest Indian Ocean is the source region of the AC and hydrographic conditions are transmitted to the Agulhas Corridor area [*Simon et al*., 2013]. Alternatively, or in addition, periods of higher salinity in the source region could also entail a greater fraction of Indian Ocean water entering the Atlantic Ocean.

We observe that high-coccolithophore productivities in the Agulhas Bank slope generally coincide with subtle increases in the Cape Basin Abundance of tropical-subtropical foraminifera (ALF) [*Peeters et al*., 2004] (periods B in Figure 6). This is especially evident just before TII, when ALF reaches its maximum (Figure 6e) and salinity on the Agulhas Bank slope sharply increased [*Marino et al*., 2013] (Figure 6f). One explanation is that ALF and salinity in the Agulhas Corridor are responding to the same changes in westerly and front position that are driving salinity changes in the AC source region and therefore correlate with productivity. However, if the higher ALF and salinity in the Agulhas Corridor are also driven in part by increased Agulhas leakage, then the productivity-promoting eddy activity associated with Agulhas leakage [*Cortese et al*., 2004] might have also contributed to enhanced productivity, in addition to westerly-modulated productivity variations.

Despite the overall correlation between productivity, ALF, and salinity in the Agulhas Corridor, the brief extreme warm and saline period during TII, immediately prior to MIS 5, does not coincide with a comparable extreme peak in productivity. We suggest that the extent of summer-autumn convection and productivity in the Agulhas Bank slope does not depend linearly on westerly location or front position. Extreme southerly positions of the westerly wind belt during obliquity maxima, such as may be recorded by ALF and salinity during TII, may not have resulted in further enhancement of water column mixing and production, as the southern influence of easterly upwelling-promoting trade winds is also constrained by the position of the SAA and South African low.

Obliquity minima coincide with maxima in $\delta^{18}O$ of *G. ruber* in the South Atlantic subtropical gyre (core 64PE-174P13). If these maxima in *G. ruber* $\delta^{18}O$ reflected predominantly colder temperatures during obliquity minima, they would be consistent with a northward displacement of westerlies and fronts, reduced salt and heat transport from Agulhas leakage [*Scussolini and Peeters*, 2013], and productivity minima in the Agulhas Bank slope.

#### 5.1.4. Pacing and Feedback in Orbital Scale Regulation of Westerlies

To date, models forced by latitudinal displacements of westerlies are able to reproduce the observed changes in hydrographical characteristics and recirculation in the southwest Indian Ocean, which may be transmitted to the Agulhas Corridor [*Simon et al*., 2013]. However, given the mounting evidence of obliquity pacing in different records from cores influenced by the AC, and potentially beyond this area [*Pena et al*., 2008], a model study to observe westerly response to extreme obliquities and observed SST is needed. The influence of SST, sea ice, and orbital forcing on the westerly distribution and intensity has been evaluated during the LGM and preindustrial times [*Sime et al*., 2013]. Yet the LGM orbital configuration is a period of intermediate obliquity, while evidence from the Southern Ocean shows that extreme cold events recorded by IRD deposition have a strong obliquity pacing over the last 265 kyr [*Marino et al*., 2013; *Simon et al*., 2013]. Models must evaluate if obliquity-driven SST changes in these sectors are sufficient to force westerlies to produce the observed changes in the strength of the southwest Indian Ocean subgyre recirculation [*Durgadoo et al*., 2013; *Simon et al*., 2013]. Extended sea ice cover has been suggested to cause an equatorward displacement of westerlies and fronts [*Chiang and Bitz*, 2005], and the regulation of summer duration by obliquity in high latitudes implies that summer sea ice may be a particularly important modulator of westerly dynamics. Unfortunately, existing sea ice proxies record predominantly winter sea ice extent

[*Gersonde et al*., 2005; *Wolff et al*., 2006]. Model studies taking into account extreme obliquity scenarios and sea ice would significantly improve our understanding of the implications for glacial $CO_2$ sequestration, since summer sea ice extent may influence the deep ocean ventilation rate, but only if a certain threshold is surpassed [*Burke et al*., 2013]. Furthermore, they would also clarify the role that changes in westerly winds might have played in imposing an obliquity pacemaker for glacial terminations.

## 6. Conclusions

Coccolith Sr/Ca ratios were used to reconstruct paleoproductivity variations in the Atlantic sector of the Southern Ocean north of the STF at core site MD96-2080 between 216 and 116 kyr. The productivity component of variation in Sr/Ca was successfully extracted from temperature and assemblage effects.

Productivity as indicated by coccolith Sr/Ca agrees well with productivity trends inferred from the relative abundance of *G. bulloides* in a nearby core in the Cape Basin and the degree of water column stratification indicated by the *F. profunda* index in MD96-2080. This suggests that productivity was driven by the degree of upper water column mixing, currently associated with summer-autumn easterly winds and that it was regulated similarly over the whole Agulhas Corridor. Since all productivity proxies are affected to some degree by secondary influences, reproducibility of trends among different types of proxies increases confidence in inferences of paleoproductivity variation. The Sr/Ca proxy adds another readily measured proxy to the paleoproductivity toolbox and provides a record of productivity directly from a primary producer with no or limited influence of preservation on the signal.

Productivity minima coincide with extreme cold events marked by deposition of IRD on the Agulhas Plateau, which may be conditioned by low obliquity. During these cold events, an extreme northerly position of the westerly wind belt and STF may have blocked the influence of upwelling-promoting easterly trade winds in the Agulhas Bank slope and decreased productivity. Periods of low productivity during low obliquity also coincide with a trend toward low salinity during obliquity minima upstream of the AC in the South Indian gyre. These salinity minima are also interpreted to reflect periods of a strengthening/northward displacement of the westerlies and a concomitant increase in recirculation of southern sourced colder/freshwaters into the Agulhas Return Current.

Our new evidence for extreme westerly latitudinal shifts inferred from productivity variation on the Agulhas Bank slope adds a new perspective to the debate on variation of westerly position during the late Quaternary. It also increases the body of evidence for an important obliquity pacing to changes in westerlies and Southern Ocean fronts, which would have implications for glacial $CO_2$ sequestration and the role of obliquity in glacial terminations.

## Author Contributions

L.M.M. prepared coccolith samples for geochemistry and measured Sr/Ca ratios; P.Z, G.M., and M.C identified coccolithophorid assemblages; G.M.M. and R.Z. generated $\delta^{13}C$ in *G. bulloides*, C.B. conducted stable isotope measurements in coccolith fraction and cross-spectral analysis. L.M.M. and H.M.S. interpreted data and wrote the paper with input from authors.

**Acknowledgments**

This investigation was funded by MICINN CGL2009-10806 (PROCARSO) and ERC 240222-PACE. L.M.M. who initiated this study with a master scholarship provided by Fundación Carolina. G.M. acknowledges financial support by the Universitat Autònoma de Barcelona (grant PS-688-01/08). R.Z. acknowledges the support of the European Community's Seventh Framework Programme FP7/2007-2013-Marie-Curie ITN, under Grant Agreement 238512, GATEWAYS project. We thank Frank Peeters for the data on foraminiferal assemblages from core GeoB-3603-2 and Andrea Burke for her useful comments on sea ice interpretations. We thank Editor Christopher Charles and an anonymous reviewer for their useful comments to improve the manuscript. Geochemical data will be available in the World Data Center for Paleoclimatology of the NOAA.

## References

Anderson, R. F., S. Ali, L. I. Bradtmiller, S. H. H. Nielsen, M. Q. Fleisher, B. E. Anderson, and L. H. Burckle (2009), Wind-driven upwelling in the Southern Ocean and the deglacial rise in atmospheric $CO_2$, *Science*, *323*(5920), 1443–8, doi:10.1126/science.1167441.

Beal, L. M., W. P. M. De Ruijter, A. Biastoch, and R. Zahn (2011), On the role of the Agulhas system in ocean circulation and climate, *Nature*, *472*(7344), 429–436, doi:10.1038/nature09983.

Beaufort, L. (1997), Insolation cycles as a major control of equatorial Indian Ocean Primary Production, *Science*, *278*(5342), 1451–1454, doi:10.1126/science.278.5342.1451.

Beaufort, L., T. de Garidel-Thoron, A. C. Mix, and N. G. Pisias (2001), ENSO-like forcing on oceanic primary production during the Late Pleistocene, *Science*, *293*(5539), 2440–2444, doi:10.1126/science.293.5539.2440.

Belkin, I. M., and A. L. Gordon (1996), Southern Ocean fronts from the Greenwich meridian to Tasmania, *J. Geophys. Res.*, *101*(C2), 3675–3696, doi:10.1029/95JC02750.

Bertrand, P., Y. Balut, R. Schneider, M.-T. Chen, J. Rogers, and Shipboard-Participants (1997), Scientific report of the NAUSICAA- IMAGES coring cruise: La Reunion October 20, 1996 - La Reunion November 25, 1996 aboard the S./V. Marion Dufresne, in *l'Institut Francais pour la Recherche et la Technologie Polaires*, *Rep. 97-1*, pp. 1–381.

Bickert, T., and G. Wefer (1996), Late Quaternary deep water circulation in the South Atlantic: reconstruction from carbonate dissolution and benthic stable isotopes, in *The South Atlantic: Present and Past Circulation*, edited by G. Wefer et al., pp. 599–620, Springer, Berlin, Heidelberg.

Boeckel, B., and K.-H. Baumann (2004), Distribution of coccoliths in surface sediments of the south-eastern South Atlantic Ocean: Ecology, preservation and carbonate contribution, *Mar. Micropaleontol.*, *51*(3-4), 301–320, doi:10.1016/j.marmicro.2004.01.001.

Bolton, C. T., and H. M. Stoll (2013), Late Miocene threshold response of marine algae to carbon dioxide limitation, *Nature*, *500*(7464), 558–62, doi:10.1038/nature12448.

Bown, P. R., and J. R. Young (1998), *Techniques in: Calcareous Nannofossil Biostratigraphy*, edited by P. R. Bown, Kluwer Academic Publishers, London.

Brown, S. J., and H. Elderfield (1996), Variations in Mg/Ca and Sr/Ca ratios of planktonic foraminifera caused by postdepositional dissolution: Evidence of shallow Mg-dependent dissolution, *Paleoceanography*, *11*(5), 543–551, doi:10.1029/96PA01491.

Burke, A., J. Adkins, R. Ferrari, L. Robinson, A. Stewart, and A. Thompson (2013), Radiocarbon and Overturning Circulation in the Glacial Southern Ocean, *paper presented at 11th International Conference on Paleoceanography*, International Conference on Paleoceanography, Sitges, Spain.

Caley, T., et al. (2011), High-latitude obliquity as a dominant forcing in the Agulhas current system, *Clim. Past*, *7*(4), 1285–1296, doi:10.5194/cp-7-1285-2011.

Chapman, M. R. (2010), Seasonal production patterns of planktonic foraminifera in the NE Atlantic Ocean: Implications for paleotemperature and hydrographic reconstructions, *Paleoceanography*, *25*, PA1101, doi:10.1029/2008PA001708.

Chapman, P., and J. L. Largier (1989), On the origin of Agulhas Bank bottom water, *S. Afr. J. Sci.*, *85*(8), 515–518.

Chiang, J. C. H., and C. M. Bitz (2005), Influence of high latitude ice cover on the marine Intertropical Convergence Zone, *Clim. Dyn.*, *25*(5), 477–496, doi:10.1007/s00382-005-0040-5.

Chiu, T.-C., and W. S. Broecker (2008), Toward better paleocarbonate ion reconstructions: New insights regarding the CaCO 3 size index, *Paleoceanography*, *23*, PA2216, doi:10.1029/2008PA001599.

Cortese, G., A. Abelmann, and R. Gersonde (2004), A glacial warm water anomaly in the subantarctic Atlantic Ocean, near the Agulhas Retroflection, *Earth Planet. Sci. Lett.*, *222*(3), 767–778, doi:10.1016/j.epsl.2004.03.029.

De Ruijter, W. P. M., A. Biastoch, S. S. Drijfhout, J. R. E. Lutjeharms, R. P. Matano, T. Pichevin, P. J. van Leeuwen, and W. Weijer (1999), Indian-Atlantic interocean exchange: Dynamics, estimation and impact, *J. Geophys. Res.*, *104*(C9), 20,885–20,910, doi:10.1029/1998JC900099.

De Villiers, S., M. Greaves, and H. Elderfield (2002), An intensity ratio calibration method for the accurate determination of Mg/Ca and Sr/Ca of marine carbonates by ICP-AES, *Geochem. Geophys. Geosyst.*, *3*(1), 1001, doi:10.1029/2001GC000169.

Dencausse, G., M. Arhan, and S. Speich (2011), Is there a continuous Subtropical Front south of Africa?, *J. Geophys. Res.*, *116*, C02027, doi:10.1029/2010JC006587.

Dudley, W. C., and D. E. Goodney (1979), Oxygen isotope content of coccoliths grown in culture, *Deep Sea Res. Part A*, *26*(5), 495–503, doi:10.1016/0198-0149(79)90092-X.

Durgadoo, J. V., B. R. Loveday, C. J. C. Reason, P. Penven, and A. Biastoch (2013), Agulhas leakage predominantly responds to the Southern Hemisphere Westerlies, *J. Phys. Oceanogr.*, *43*(10), 2113–2131, doi:10.1175/JPO-D-13-047.1.

Esper, O., G. J. M. Versteegh, K. A. F. Zonneveld, and H. Willems (2004), A palynological reconstruction of the Agulhas Retroflection (South Atlantic Ocean) during the Late Quaternary, *Global Planet. Change*, *41*(1), 31–62, doi:10.1016/j.gloplacha.2003.10.002.

Fink, C., K.-H. Baumann, J. Groeneveld, and S. Steinke (2010), Strontium/Calcium ratio, carbon and oxygen stable isotopes in coccolith carbonate from different grain-size fractions in South Atlantic surface sediments, *Geobios*, *43*(1), 151–164, doi:10.1016/j.geobios.2009.11.001.

Ganssen, G. M., and D. Kroon (2000), The isotopic signature of planktonic foraminifera from NE Atlantic surface sediments: Implications for the reconstruction of past oceanic conditions, *J. Geol. Soc.*, *157*(3), 693–699, doi:10.1144/jgs.157.3.693.

Gersonde, R., X. Crosta, A. Abelmann, and L. Armand (2005), Sea-surface temperature and sea ice distribution of the Southern Ocean at the EPILOG Last Glacial Maximum—A circum-Antarctic view based on siliceous microfossil records, *Quat. Sci. Rev.*, *24*(7), 869–896, doi:10.1016/j.quascirev.2004.07.015.

Gordon, A. L., J. R. E. Lutjeharms, and M. L. Gründlingh (1987), Stratification and circulation at the Agulhas Retroflection, *Deep Sea Res. Part A*, *34*(4), 565–599, doi:10.1016/0198-0149(87)90006-9.

Grelaud, M., G. Marino, P. Ziveri, and E. J. Rohling (2012), Abrupt shoaling of the nutricline in response to massive freshwater flooding at the onset of the last interglacial sapropel event, *Paleoceanography*, *27*, PA3208, doi:10.1029/2012PA002288.

Hodell, D. A., K. A. Venz, C. D. Charles, and U. S. Ninnemann (2003), Pleistocene vertical carbon isotope and carbonate gradients in the South Atlantic sector of the Southern Ocean, *Geochem. Geophys. Geosyst.*, *4*(1), 1004, doi:10.1029/2002GC000367.

Jury, M. R. (2011), Environmental Influences on South African Fish Catch: South Coast Transition, *Int. J. Oceanogr.*, *2011*, 1–10, doi:10.1155/2011/920414.

Kohfeld, K. E., R. M. Graham, A. M. de Boer, L. C. Sime, E. W. Wolff, C. Le Quéré, and L. Bopp (2013), Southern Hemisphere westerly wind changes during the Last Glacial Maximum: Paleo-data synthesis, *Quat. Sci. Rev.*, *68*, 76–95, doi:10.1016/j.quascirev.2013.01.017.

Langer, G., N. Gussone, G. Nehrke, U. Riebesell, A. Eisenhauer, H. Kuhnert, B. Rost, S. Trimborn, and S. Thoms (2006), Coccolith strontium to calcium ratios in Emiliania huxleyi: The dependence on seawater strontium and calcium concentrations, *Limnol. Oceanogr.*, *51*(1), 310–320, doi:10.4319/lo.2006.51.1.0310.

Largier, J. L., P. Chapman, W. T. Peterson, and V. P. Swart (1992), The western Agulhas Bank: circulation, stratification and ecology, *S. Afr. J. Mar. Sci.*, *12*(1), 319–339, doi:10.2989/02577619209504709.

Lutjeharms, J. R. E. (2006), *The Agulhas Current*, Springer-Verlag, Würzburg, Bayern.

Lutjeharms, J. R., and R. C. van Ballegooyen (1988), Anomalous upstream retroflection in the agulhas current, *Science*, *240*(4860), 1770, doi:10.1126/science.240.4860.1770.

Marino, G., R. Zahn, M. Ziegler, C. Purcell, G. Knorr, I. R. Hall, P. Ziveri, and H. Elderfield (2013), Agulhas salt-leakage oscillations during abrupt climate changes of the Late Pleistocene, *Paleoceanography*, *28*, 1–8, doi:10.1002/palo.20038.

Martínez-Méndez, G., R. Zahn, I. R. Hall, L. D. Pena, and I. Cacho (2008), 345,000-year-long multi-proxy records off South Africa document variable contributions of Northern versus Southern Component Water to the Deep South Atlantic, *Earth Planet. Sci. Lett.*, *267*(1), 309–321, doi:10.1016/j.epsl.2007.11.050.

Martínez-Méndez, G., E. G. Molyneux, I. R. Hall, and R. Zahn (2009), Variable water column structure of the South Atlantic on glacial–interglacial time scales, *Quat. Sci. Rev.*, *28*(27), 3379–3387, doi:10.1016/j.quascirev.2009.09.022.

Martínez-Méndez, G., R. Zahn, I. R. Hall, F. J. C. Peeters, L. D. Pena, I. Cacho, and C. Negre (2010), Contrasting multiproxy reconstructions of surface ocean hydrography in the Agulhas Corridor and implications for the Agulhas Leakage during the last 345,000 years, *Paleoceanography*, *25*, PA4227, doi:10.1029/2009PA001879.

Mortyn, P. G., and C. D. Charles (2003), Planktonic foraminiferal depth habitat and δ18O calibrations: Plankton tow results from the Atlantic sector of the Southern Ocean, *Paleoceanography*, *18*(2), 1037, doi:10.1029/2001PA000637.

Müller, M. N., M. Lebrato, U. Riebesell, J. Barcelos e Ramos, K. G. Schulz, S. Blanco-Ameijeiras, S. Sett, A. Eisenhauer, and H. M. Stoll (2014), Influence of temperature and CO2 on the strontium and magnesium composition of coccolithophore calcite, *Biogeosciences*, *11*(4), 1065–1075, doi:10.5194/bg-11-1065-2014.

Nianqiao, F., C. Xuefang, D. Xuan, H. Chaoyong, Y. Yong, and N. Haogang (2001), Paleoceanographical records under impact of the Indian monsoon from the Bengal Deep Sea Fan and Ninetyeast Ridge during the last 260 ka, *Sci. China, Ser. D Earth Sci.*, *44*, 351–359, doi:10.1007/BF02912006.

Orsi, A. H., T. Whitworth, and W. D. Nowlin (1995), On the meridional extent and fronts of the Antarctic Circumpolar Current, *Deep Sea Res. Part I*, *42*(5), 641–673, doi:10.1016/0967-0637(95)00021-W.

Pahnke, K., and R. Zahn (2005), Southern Hemisphere water mass conversion linked with North Atlantic climate variability, *Science*, *307*(5716), 1741–6, doi:10.1126/science.1102163.

Pahnke, K., R. Zahn, H. Elderfield, and M. Schulz (2003), 340,000-year centennial-scale marine record of Southern Hemisphere climatic oscillation, *Science*, *301*(5635), 948–52, doi:10.1126/science.1084451.

Peeters, F. J. C., R. Acheson, G.-J. A. Brummer, W. P. M. De Ruijter, R. R. Schneider, G. M. Ganssen, E. Ufkes, and D. Kroon (2004), Vigorous exchange between the Indian and Atlantic oceans at the end of the past five glacial periods, *Nature*, *430*(7000), 661–5, doi:10.1038/nature02785.

Pena, L. D., I. Cacho, P. Ferretti, and M. A. Hall (2008), El Niño-Southern Oscillation-like variability during glacial terminations and interlatitudinal teleconnections, *Paleoceanography*, *23*, PA3101, doi:10.1029/2008PA001620.

Rau, A. J., J. Rogers, J. R. E. Lutjeharms, J. Giraudeau, J. A. Lee-Thorp, M.-T. Chen, and C. Waelbroeck (2002), A 450-kyr record of hydrological conditions on the western Agulhas Bank Slope, south of Africa, *Mar. Geol.*, *180*(1-4), 183–201, doi:10.1016/S0025-3227(01)00213-4.

Reason, C. J. C., J. R. E. Lutjeharms, J. Hermes, A. Biastoch, and R. E. Roman (2003), Inter-ocean fluxes south of Africa in an eddy-permitting model, *Deep Sea Res. Part II*, *50*(1), 281–298, doi:10.1016/S0967-0645(02)00385-5.

Reichart, G.-J., and H. Brinkhuis (2003), Late Quaternary Protoperidinium cysts as indicators of paleoproductivity in the northern Arabian Sea, *Mar. Micropaleontol.*, *49*(4), 303–315, doi:10.1016/S0377-8398(03)00050-1.

Reynolds, R. W., and T. M. Smith (1994), Improved global sea surface temperature analyses using optimum interpolation, *J. Climate*, *7*, 929–948, doi:10.1175/1520-0442(1994)007<0929:IGSSTA>2.0.CO;2.

Rickaby, R. E. M., D. P. Schrag, I. Zondervan, and U. Riebesell (2002), Growth rate dependence of Sr incorporation during calcification of Emiliania huxleyi, *Global Biogeochem. Cycles*, *16*(1), 1006, doi:10.1029/2001GB001408.

Rykaczewski, R. R., and D. M. Checkley (2008), Influence of ocean winds on the pelagic ecosystem in upwelling regions, *Proc. Natl. Acad. Sci. U. S. A.*, *105*(6), 1965–70, doi:10.1073/pnas.0711777105.

Salgueiro, E., et al. (2008), Planktonic foraminifera from modern sediments reflect upwelling patterns off Iberia: Insights from a regional transfer function, *Mar. Micropaleontol.*, *66*(3), 135–164, doi:10.1016/j.marmicro.2007.09.003.

Schumann, E. H., A. L. Cohen, and M. R. Jury (1995), Coastal sea surface temperature variability along the south coast of South Africa and the relationship to regional and global climate, *J. Mar. Res.*, *53*(2), 231–248, doi:10.1357/0022240953213205.

Scussolini, P., and F. J. C. Peeters (2013), A record of the last 460 thousand years of upper ocean stratification from the central Walvis Ridge, South Atlantic, *Paleoceanography*, *28*, 1–14, doi:10.1002/palo.20041.

Sime, L. C., K. E. Kohfeld, C. Le Quéré, E. W. Wolff, A. M. de Boer, R. M. Graham, and L. Bopp (2013), Southern Hemisphere westerly wind changes during the Last Glacial Maximum: model-data comparison, *Quat. Sci. Rev.*, *64*, 104–120, doi:10.1016/j.quascirev.2012.12.008.

Simon, M. H., K. L. Arthur, I. R. Hall, F. J. C. Peeters, B. R. Loveday, S. Barker, M. Ziegler, and R. Zahn (2013), Millennial-scale Agulhas Current variability and its implications for salt-leakage through the Indian–Atlantic Ocean Gateway, *Earth Planet. Sci. Lett.*, *383*, 101–112, doi:10.1016/j.epsl.2013.09.035.

Stoll, H. M., and P. Ziveri (2002), Separation of monospecific and restricted coccolith assemblages from sediments using differential settling velocity, *Mar. Micropaleontol.*, *46*(1), 209–221, doi:10.1016/S0377-8398(02)00040-3.

Stoll, H. M., C. M. Klaas, I. Probert, J. Ruiz Encinar, and J. I. Garcia Alonso (2002a), Calcification rate and temperature effects on Sr partitioning in coccoliths of multiple species of coccolithophorids in culture, *Global Planet. Change*, *34*(3), 153–171, doi:10.1016/S0921-8181(02)00112-1.

Stoll, H. M., Y. Rosenthal, and P. Falkowski (2002b), Climate proxies from Sr/Ca of coccolith calcite: Calibrations from continuous culture of Emiliania huxleyi, *Geochim. Cosmochim. Acta*, *66*(6), 927–936, doi:10.1016/S0016-7037(01)00836-5.

Stoll, H. M., P. Ziveri, M. Geisen, I. Probert, and J. R. Young (2002c), Potential and limitations of Sr/Ca ratios in coccolith carbonate: new perspectives from cultures and monospecific samples from sediments, *Philos. Trans. R. Soc. London, Ser. A*, *360*(1793), 719–47, doi:10.1098/rsta.2001.0966.

Stoll, H. M., N. Shimizu, A. Arevalos, N. Matell, A. Banasiak, and S. Zeren (2007a), Insights on coccolith chemistry from a new ion probe method for analysis of individually picked coccoliths, *Geochem. Geophys. Geosyst.*, *8*, Q06020, doi:10.1029/2006GC001546.

Stoll, H. M., N. Shimizu, D. Archer, and P. Ziveri (2007b), Coccolithophore productivity response to greenhouse event of the Paleocene–Eocene Thermal Maximum, *Earth Planet. Sci. Lett.*, *258*(1), 192–206.

Stoll, H. M., P. Ziveri, N. Shimizu, M. Conte, and S. Theroux (2007c), Relationship between coccolith Sr/Ca ratios and coccolithophore production and export in the Arabian Sea and Sargasso Sea, *Deep Sea Res. Part II*, *54*, 581–600, doi:10.1016/j.dsr2.2007.01.003.

Stoll, H. M., A. Arevalos, A. Burke, P. Ziveri, G. Mortyn, N. Shimizu, and D. Unger (2007d), Seasonal cycles in biogenic production and export in Northern Bay of Bengal sediment traps, *Deep Sea Res. Part II*, *54*, 558–580, doi:10.1016/j.dsr2.2007.01.002.

Toggweiler, J. R., J. L. Russell, and S. R. Carson (2006), Midlatitude westerlies, atmospheric $CO_2$, and climate change during the ice ages, *Paleoceanography*, *21*, PA2005, doi:10.1029/2005PA001154.

Trenberth, K. E., J. G. Olson, and W. G. Large (1989), A Global Ocean Wind Stress Climatology based on ECMWF Analyses, *NCAR Tech. Note NCAR/TN-338+STR*, doi:10.5065/D6ST7MR9.

Valentine, H. R., J. R. E. Lutjeharms, and G. B. Brundrit (1993), The water masses and volumetry of the southern Agulhas Current region, *Deep Sea Res. Part I*, *40*(6), 1285–1305, doi:10.1016/0967-0637(93)90138-S.

West, S., J. H. F. Jansen, and J.-B. Stuut (2004), Surface water conditions in the Northern Benguela Region (SE Atlantic) during the last 450 ky reconstructed from assemblages of planktonic foraminifera, *Mar. Micropaleontol.*, *51*(3), 321–344, doi:10.1016/j.marmicro.2004.01.004.

Wilke, I., H. Meggers, and T. Bickert (2009), Depth habitats and seasonal distributions of recent planktic foraminifers in the Canary Islands region (29°N) based on oxygen isotopes, *Deep Sea Res. Part I*, *56*(1), 89–106, doi:10.1016/j.dsr.2008.08.001.

Wolff, E. W., et al. (2006), Southern Ocean sea-ice extent, productivity and iron flux over the past eight glacial cycles, *Nature*, *440*(7083), 491–496, doi:10.1038/nature04614.

Young, J. R., and P. Ziveri (2000), Calculation of coccolith volume and it use in calibration of carbonate flux estimates, *Deep Sea Res. Part II*, *47*(9), 1679–1700, doi:10.1016/S0967-0645(00)00003-5.

Young, J. R., M. Geisen, L. Cros, A. Kleijne, C. Sprengel, I. Probert, and J. Ostergaard (2003), A guide to extant coccolithophore taxonomy, *J. Nannoplankton Res.*, *Special Issue*, *1*, 1–125.

Ziegler, M., P. Diz, I. R. Hall, and R. Zahn (2013), Millennial-scale changes in atmospheric $CO_2$ levels linked to the Southern Ocean carbon isotope gradient and dust flux, *Nat. Geosci.*, *6*(6), 457–461, doi:10.1038/ngeo1782.

Ziveri, P., H. Stoll, I. Probert, C. Klaas, M. Geisen, G. Ganssen, and J. Young (2003), Stable isotope "vital effects" in coccolith calcite, *Earth Planet. Sci. Lett.*, *210*(1), 137–149, doi:10.1016/S0012-821X(03)00101-8.